# The effect of gradation on the response of saturated sands when subjected to seismic loading: A centrifuge test



Trevor J. Carey
Assistant Professor, Department of Civil Engineering
University of British Columbia, Vancouver, BC, Canada,
ticarey@ucdavis.edu

## Anna Chiaradonna

Research Assistant, Department of Civil, Construction, Architectural, and Environmental Engineering University of L'Aquila, 19 Piazza Santa Margherita, 2 Palazzo Camponeschi, 67100 L'Aquila AQ, Italy, anna.chiaradonna1@univaq.it

#### Nathan Love

Ph.D. Student, Department of Civil & Environmental Engineering University of California at Davis, One Shields Ave., Davis, CA USA, 95616, nclove@ucdavis.edu

Jason T. DeJong

Professor, Department of

Professor, Department of Civil & Environmental Engineering University of California at Davis, One Shields Ave., Davis, CA USA, 95616, jdejong@ucdavis.edu

## Katerina Ziotopoulou

Assistant Professor, Department of Civil & Environmental Engineering University of California at Davis, One Shields Ave., Davis, CA USA. 95616. kziotopoulou@ucdavis.edu

### **ABSTRACT**

The standard of practice when assessing the liquefaction susceptibility of geosystems uses an empirical case history database that was primarily developed for clean, poorly graded sands. However, many geosystems in the built environment are either constructed with or founded on well graded soils, creating a disconnect between the sand encountered in practice and the sand used as the basis of knowledge. Using the 9-m centrifuge at the University of California Davis's Center for Geotechnical Modeling a centrifuge experiment was designed to test the dynamic response of embankments constructed poorly graded and well graded sands at the system level scale. The experiment consisted of two 10-degree slopes, one constructed with a poorly graded sand and the other with a well graded sand positioned side by side in the same model container. Each slope was dry pluviated to the same relative density of D<sub>r</sub>=63%, while the absolute densities were different. The slopes were instrumented with dense arrays of pore pressure transducers and accelerometers in the level ground at the head of the slope. The stress-strain behavior between accelerometers was calculated using inverse analysis techniques, providing a 1-D shear-beam soil response at the sensor array location. Liquefaction was triggered, as defined by an excess porewater pressure ratio (ru) of 1.0, but the shear strains at triggering in the well graded sand were significantly less than the strains in the poorly graded sand. During cyclic mobility, strain accumulation in the well graded sand occurred at a slower rate. This study demonstrates that liquefaction triggering and the post-triggering response for saturated sands needs to consider gradation characteristics and clean poorly graded sands cannot act as a single predictor of dynamic response for all sand gradations.

#### RÉSUMÉ

La pratique standard de l'évaluation de la susceptibilité de liquéfaction des géosystèmes implique l'utilisation d'une base de données historiques tirées de cas empiriques, développée principalement pour des sables fins à granulométrie irrégulière. Toutefois, plusieurs géosystèmes dans l'environnement bâti sont soit construits, soit fondés sur des sables a granulométrie régulière, générant ainsi une incohérence entre le sable trouvé dans la pratique et le sable utilisé comme référence. Une expérience de centrifugation mettant en œuvre la centrifugeuse de 9 m au Davis's Center for Geotechnical Modeling de l'université de Californie a été conçue afin de tester la réponse dynamique des sables a granulométrie régulière et irrégulière des remblais à l'échelle du système. L'expérience portait sur deux pentes de 10 degrés, l'une construite avec du sable à granulométrie irrégulière et l'autre avec du sable à granulométrie régulière, positionnées l'une à côté de l'autre dans le même contenant. Chaque pente fut constituée par pluviation à sec, de densité relative identique (D<sub>r</sub>=63%) et de densités absolues différentes. Les pentes furent équipées d'un réseau dense de transducteurs de pression

interstitielle et d'accéléromètres à la tête de la pente et à mi-pente. Le comportement de tension-effort entre les accéléromètres fut calculé au moyen d'une technique d'analyse inverse, fournissant une réponse de cisaillement de poutre en 1D au niveau du réseau. La liquéfaction fut déclenchée dans les deux pentes, selon la définition du taux de pression interstitielle en excès (ru) de 1,0. Mais au moment de déclencher le cisaillement, les efforts dans le sable a granulométrie régulière étaient beaucoup moins importants que dans le sable a granulométrie irrégulière. Durant la mobilité cyclique, l'accumulation de l'effort dans le sable à granulométrie régulière était plus lente que pour le sable à granulométrie irrégulière. La présente étude démontre que la réponse à la liquéfaction et la réponse post-déclenchement pour des sables saturés doivent considérer les caractéristiques de granulométrie et que les sables propres à granulométrie irrégulière ne peuvent pas se comporter comme un prédicateur simple de la réponse dynamique de toutes les granulométries de sable.

#### 1 INTRODUCTION

The standard of practice during the seismic assessment of geosystems is to use the empirical case history database that was primarily developed from observations of liquefaction at sites consisting of relatively clean poorly graded sands. The narrow range of gradation characteristics in this database poses a challenge during the seismic assessment of embankments, which are commonly constructed with or founded on more broadly graded soils. This creates a gap between the knowledge of liquefaction triggering and the soils found in the built environment, often leading to an assumption that well graded and poorly graded sands have similar dynamic behaviors during earthquake shaking.

Liquefaction of well graded or gravelly sites has been documented by others (e.g., Andrus and Youd, 1987, Towhata et al. 2014) but the case history data is limited. A recent study by Ghafghazi and DeJong (2016) reviewed and reevaluated gravelly and well graded soil liquefaction case history data and found the data generally followed the clean sand triggering curve by Boulanger and Idriss (2014). However, Ghafghazi and DeJong (2016) noted that the limited number of observations of liquefaction in well graded soils prohibited the development of reliable liquefaction assessment criteria that could be broadly applied for a range of soil gradations.

A centrifuge experiment was designed to study the effect of sand gradation on the dynamic response of a system using the 9-m centrifuge at the University of California Davis's Center for Geotechnical Modeling (CGM). The experiment consisted of two submerged embankments, dry pluviated to the same relative density of D<sub>r</sub>=63%, positioned side-by-side in a rigid model container, with one embankment constructed with a poorly graded sand and the other with a well graded sand. Earthquake shaking was simulated using a 1 Hz motion input at the base of the model container. The embankments were identically instrumented with a dense array of accelerometers and porewater pressure transducers directly below the upper bench. This paper describes the process to calculate and interpret the stress-strain responses of pseudo-elements using the centrifuge test data and inverse analysis procedures. The pseudoelements, located between adjacent accelerometers, better represent embankment in-situ and loading conditions that cannot be simulated using standard laboratory testing, providing a more complete understanding of the pre- and post- liquefaction triggering responses. Time correlated excess porewater pressure

measurements from the center of the elements are used to evaluate when liquefaction is triggered.

#### 2 SOILS AND TEST DESIGN

The two test sands for this study were sourced from an alluvial deposit from the Cape May Formation near Mauricetown, New Jersey. Post-dredging modifications were minimized and thus the particle size, shape, and mineralogy were consistent with naturally deposited sands in the built environment (Sturm 2019).

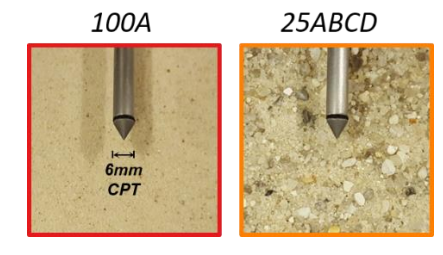


Figure 1: Photos of test sands with a 6 mm diameter CPT for scale

Photographs of the two test sands with a 6 mm CPT shown for scale are provided in Figure 1 and the particle size distributions are illustrated in Figure 2. The poorly graded 100A sand is a uniform mixture and the well graded 25ABCD sand is manufactured using 25% mass proportions of four poorly graded sands. Summarized in Table 1 are select index properties for the sands, along with the void ratios at the testing relative density of  $D_r$ =63%. The hydraulic conductivity was measured using a falling head permeability test in the laboratory, with k=0.01 cm/sec measured for 25ABCD and 0.02 cm/s for 100A sand. Additional physical and mechanical properties of the sands are provided by Sturm (2019).

The centrifuge experiment was designed and tested using the 9-m radius centrifuge at the UC Davis's Center for Geotechnical Modeling. The test was performed with a centrifugal acceleration of 40 g and followed conventional scaling laws for gravity (Garnier et al. 2007). The model was saturated under vacuum using Hydroxypropyl methylcellulose to a viscosity ( $\mu$ \*) of 40 cSt to match the centrifugal acceleration and minimize scaling conflicts during diffusion of excess porewater pressures.

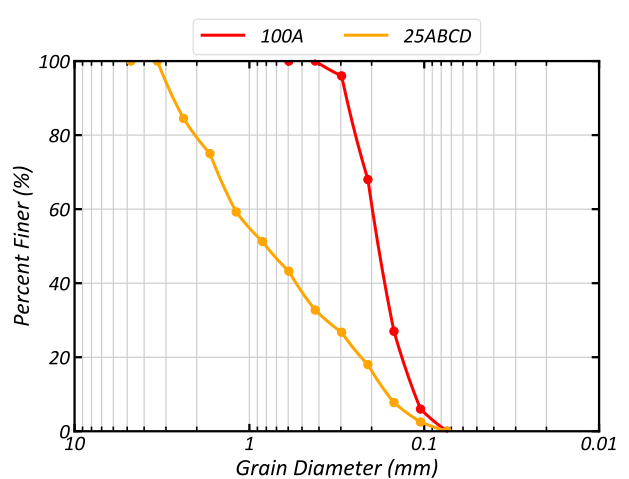


Figure 2: Particle size distributions of the two test sands

Table 1: Index properties of test sands

Sand	e <sub>min</sub>	e <sub>max</sub>	e @ D <sub>r</sub> =63%	D <sub>50</sub> (mm)	Cu	Gs
100A	0.579	0.881	0.69	0.18	1.68	2.62
25ABCD	0.303	0.544	0.39	0.80	7.44	2.61

The elevation view of the test design schematic is given in Figure 4 in model scale units. The two 10-degree submerged embankments were constructed side-by-side in the same rigid model container, separated by an Aluminum wall, with one embankment constructed with 100A sand and the other with 25ABCD sand. The geometry and instrumentation for the two embankments were identical. At the centrifugal acceleration of 40 g, the bench is 19.8 m in length and have depths of 14 and 8 m. A vertical array of accelerometers and porewater pressure transducers was located in the level ground at the head of the slope to track the soil response during shaking. The embankments were consecutively constructed using dry pluviation by raining sand down from above.

The ground motion used to simulate earthquake shaking consisted of 20 non-uniform 1 Hz (prototype scale) cycles. The motion was applied as a displacement time history at the base of the model container and accelerations propagated through the soil. In Figure 3 the recorded acceleration trace of the input motion used to generate liquefaction is provided. The motion, with a PGA of 0.23 g and an Arias intensity of 1.46 m/s, sequentially consisted of 3 cycles of building amplitude, 5 cycles of constant amplitude close to the PGA, and 12 cycles of exponential decay. The motion in Figure 3 caused both embankments to have high excess porewater pressures, which resulted in the triggering of liquefaction, and cyclic mobility with continued shaking.

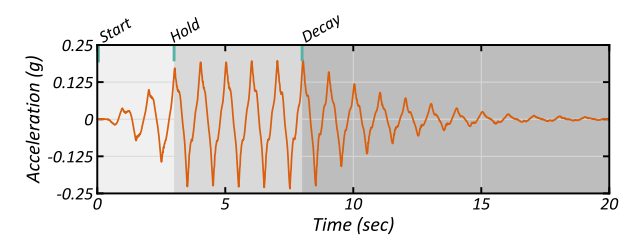


Figure 3: 1 Hz motion applied to the base of the centrifuge model to simulate earthquake shaking

# 3 STRESS-STRAIN RESPONSE OF PSEUDO-ELEMENTS

Recorded accelerations from the sensor array can be postprocessed using inverse analysis approaches to generate stress-strain responses for pseudo-elements in each embankment. The use of pseudo-elements is in-lieu of measuring stress and strain responses using traditional laboratory approaches, which cannot be performed in a centrifuge experiment. The pseudo-elements' response is valuable when relating soil element behavior to the performance of a system during earthquake shaking since the elements already include complex loading conditions (e.g. accelerations and velocities), and transient changes in stiffness from the dilating soil (Kutter and Wilson 1999) or upward seepage, which cannot be replicated using standard laboratory element testing approaches. Additionally, responses from the pseudo-elements can be used in numerical model calibration routines.

The procedure to compute dynamic shear strain ( $\gamma$ ) and shear stress ( $\tau$ ) are outlined by Brandenberg et al. (2009) and Kamai & Boulanger (2010) respectively, and assume a 1-D shear-beam response, with upward propagation of shear waves to the soil surface. The calculations performed assume a pseudo-element is located between adjacent accelerometers.

## 3.1 Calculation of Shear Stresses

Shear stresses are calculated by summing the horizontal inertial forces above the midpoint of a pseudo-element. It is assumed that accelerations within an element vary linearly between accelerometers, and shear stresses at the soil surface are zero. Soil above the near surface accelerometer is assumed to act as a rigid body (i.e. accelerations within the element are constant). The expression to calculate shear-stresses in the top pseudo-element is given in Equation 1 and the second element in Equation 2, where  $\rho$  is the saturated density of the soil, z is the depth accelerometer a.

$$\tau_1 = \rho \cdot \frac{z_1}{2} \cdot a_1 \tag{1}$$

$$\tau_2 = \tau_1 + \rho \cdot \frac{z_1}{2} \cdot a_1 + \frac{z_2 - z_1}{2} \cdot \left(\frac{3 \cdot a_1 + a_2}{4}\right)$$
 [2]

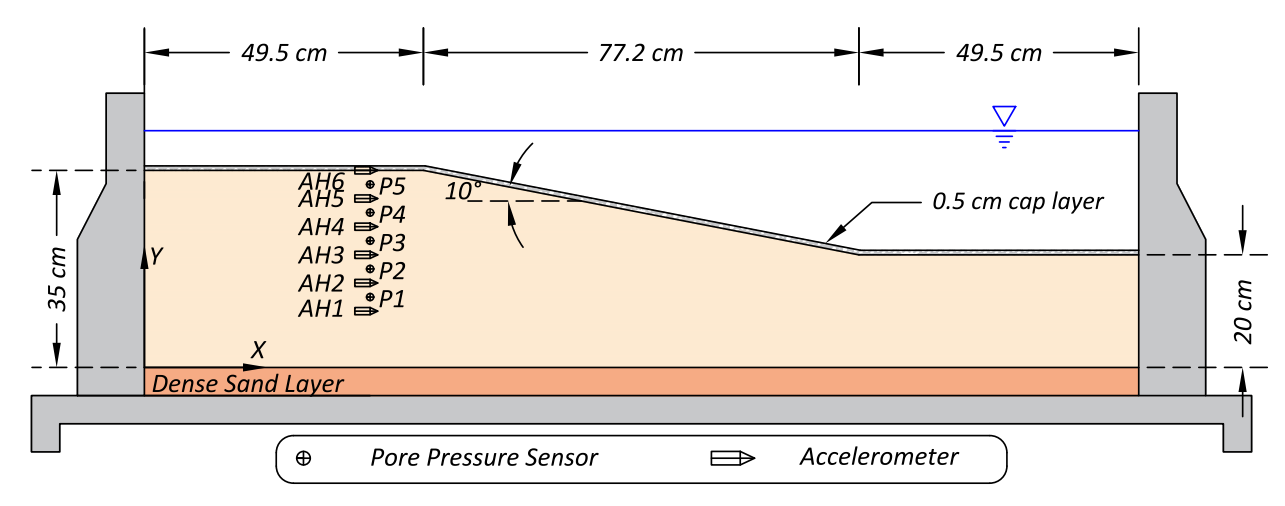


Figure 4: Elevation view of the centrifuge experiment in model scale units

#### 3.2 Calculation of Shear Strains

Dynamic shear strains are calculated using a weighted residual scheme, which is often used in finite element formulations. The weighted residual is given in Equation 3. Each accelerometer with depth z was double integrated to obtain displacement of d.

$$\begin{pmatrix}
d(t)_{2} - d(t)_{1} \\
d(t)_{3} - d(t)_{1} \\
d(t)_{3} - d(t)_{2}
\end{pmatrix}$$

$$= \frac{1}{3} \begin{bmatrix}
2(z_{2} - z_{1}) & z_{2} - z_{1} & 0 \\
z_{2} - z_{1} & 2(z_{3} - z_{1}) & z_{3} - z_{2} \\
0 & z_{3} - z_{2} & 2(z_{3} - z_{2})
\end{bmatrix} \begin{pmatrix}
\gamma(t)_{12} \\
\gamma(t)_{13} \\
\gamma(t)_{23}
\end{pmatrix}$$
[3]

# 4 RESULTS

Stress-strain responses are computed for the two shallowest elements in the level ground for each embankment. In the level ground there is no initial static shear stress that would influence soil behavior. Provided in Figure 5 are the pseudo-element locations shown with the relevant sensors for reference. Porewater pressure transducers located at the midpoint of the elements are used to evaluate when liquefaction is triggered, as defined by an excess porewater pressure ratio of 1 (ru=1), and provide a cross reference of observed dilation from the stress-strain responses.

Figures 6 and 7 present the excess porewater pressures measured by P5 and P4 (subplots a, b), the computed stress-strain for pseudo-elements 5-6 and 4-5 (subplots c, d), and computed strain for the pseudo-elements 5-6 and 4-5 as a function of time (subplots e, f). The dashed lines in the porewater pressure response correspond to the excess porewater pressure at that sensor depth that results in an  $r_u$ =1.0. The labeled green tick marks in subplot a (unlabeled in subplots b, e, f) indicate the beginning, constant amplitude cycles, exponential decay cycles, and the end of the earthquake

motion. The color gradients in subplots a-d are correlated in time.

The dynamic response for the 100A sand is presented in Figure 6. Excess porewater pressures build rapidly, triggering liquefaction (r<sub>u</sub>=1.0) at about 5 seconds, roughly the beginning of the constant amplitude cycles of shaking. Following liquefaction triggering, both elements experience large magnitudes of straining over 1-2 cycles. The peak dynamic shear strains during these cycles are about 3.4% and 2.0% for elements 5-6 and 4-5, respectively. At about 7.5 seconds the sand has softened, indicated by the flat CSR response, and can no longer transmit shear stresses. High excess porewater pressures are maintained following triggering and no significant drops in pressure occur that would indicate the soil is strongly dilating. The reduced soil stiffness lengthens the fundamental period of the element, and in turn, reduces the effect the 1 Hz input motion has on the soil since the system can no longer respond to the relatively higher frequency. The diminished effect of the input motion is a potential reason why the soil does not experience larger strains during cyclic mobility.

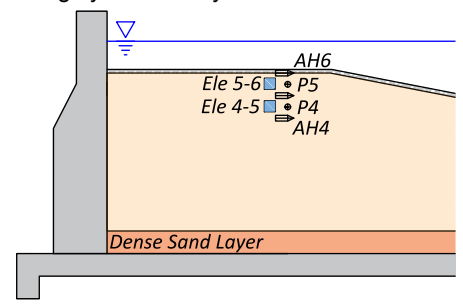


Figure 5: Location of the 5-6 and 4-5 pseudo-elements in the level ground sensor array, aligned with the pore pressure transducers

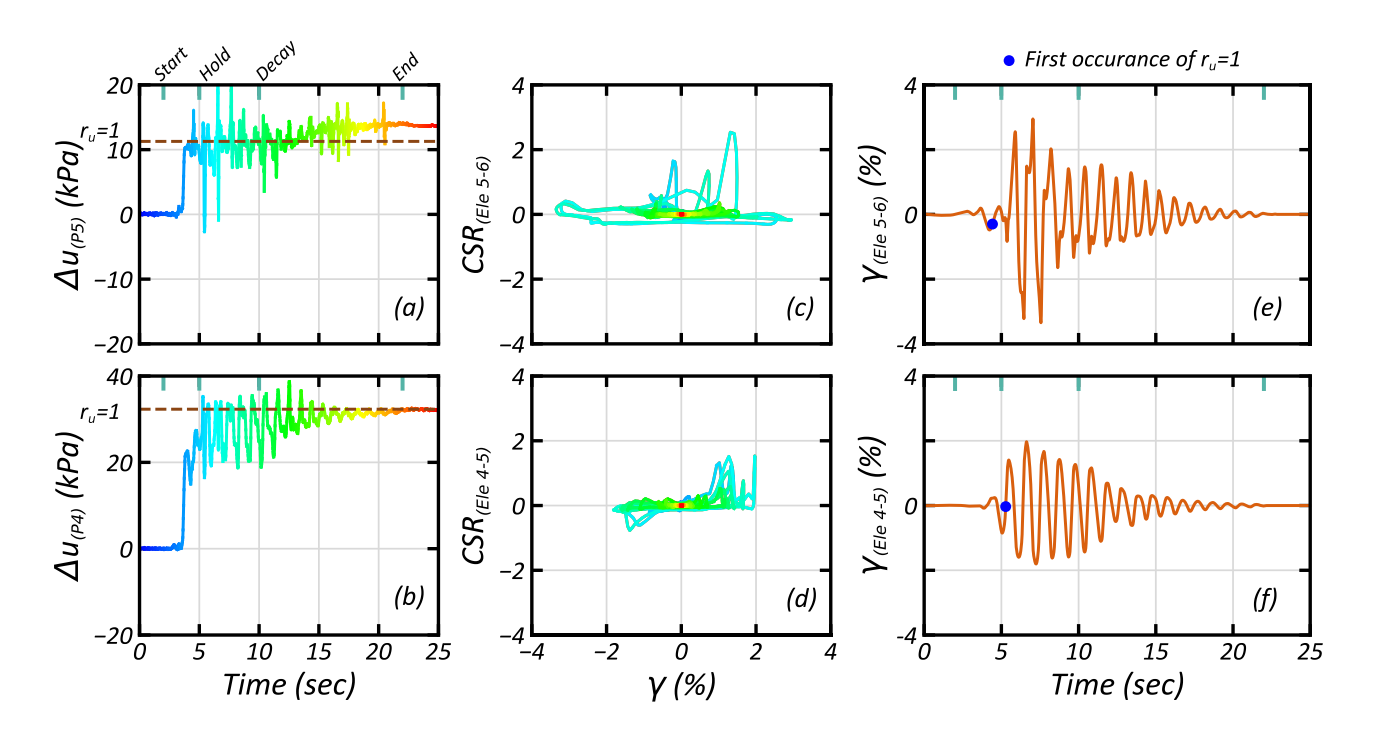


Figure 6: Level ground dynamic response for the 100A embankment including excess porewater pressures and  $r_u$  limits (subplots a and b), stress strain response of the pseudo-elements (c and d), and dynamic strains as a function of time (e and f).

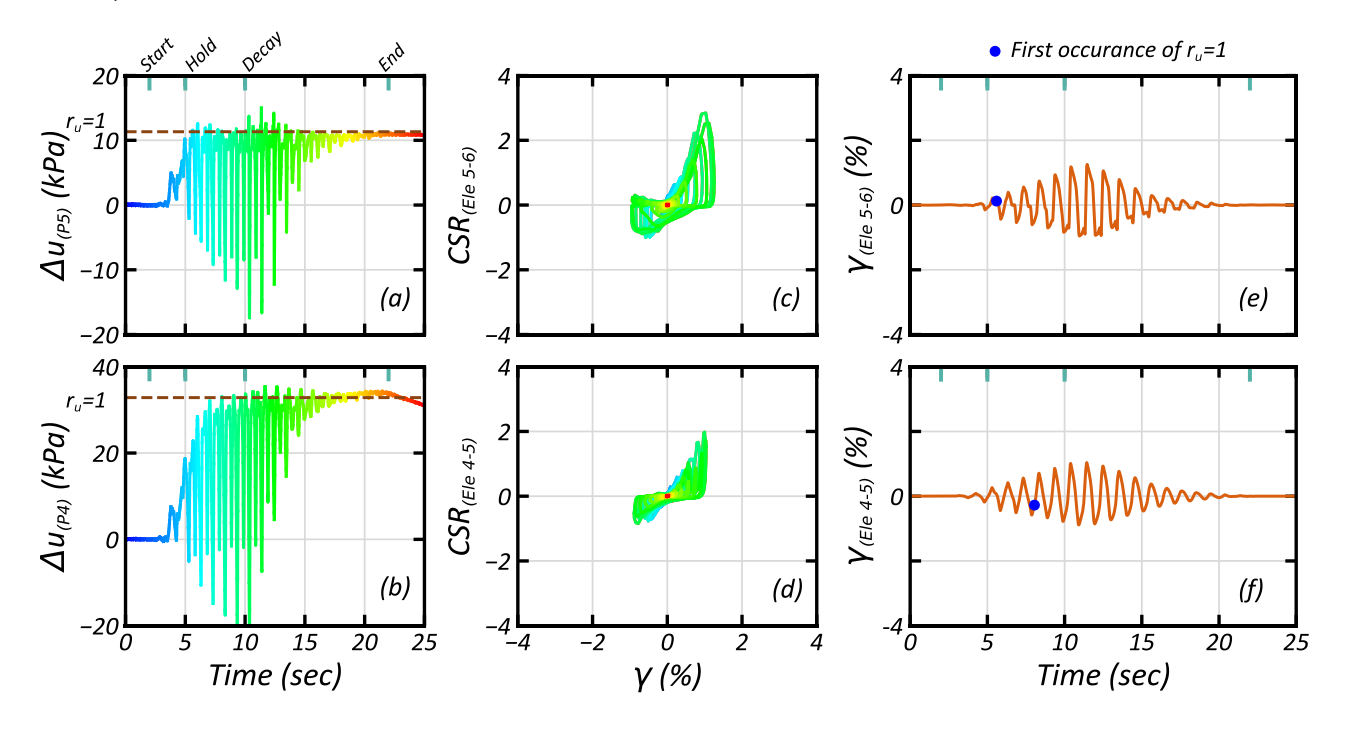


Figure 7: Level ground dynamic response for the 25ABCD embankment including excess porewater pressures and  $r_u$  limits (subplots a and b), stress strain response of the pseudo-elements (c and d), and dynamic strains as a function of time (e and f).

The dynamic response for the 25ABCD sand is provided in Figure 7. At P5 the excess porewater ratio reaches a value of 1.0 at a little over 5 seconds. Excess porewater pressures build at a slower rate for P4 in this soil, and liquefaction is not triggered until about 8 seconds. Following liquefaction triggering both elements maintain shear stiffness, allowing the soil to transmit shear stresses, indicated by the non-zero CSR in subplots c and d. During cycling, there are sharp drops and recoveries in excess porewater pressures at both P4 and P5 as the sand dilates, reducing the duration that high porewater pressures are maintained and resisting additional shear straining. The maximum shear strains in both elements does not concurrently occur with the triggering of liquefaction, but rather at the end of the constant amplitude cycles of the input motion at about 11.5 seconds. The maximum shear strains in the soil are roughly 1.25% and 0.75% for elements 5-6 and 4-5 respectively.

#### 5 DISCUSSION

Liquefaction was triggered in both the 100A and 25ABCD sands within 5-8 cycles of loading. However, the two sands have divergent post-triggering responses. The peak shear strain in the 100A sand roughly coincides with liquefaction triggering and in a single loading cycle 2.25% shear strain is accumulated for element 5-6 (Figure 6e). In the same element for the 25ABCD sand, strains accumulate linearly at a rate of about 0.2% per cycle and decrease in magnitude as the input motion intensity also decreases. The total shear strain in the 25ABCD element 5-6 is 1.25%.

The cause for the reduced strain accumulation in the 25ABCD sand is from its stronger stress-dilatancy behavior. The porewater pressure response in the 25ABCD sand shows more frequent and larger drops in excess porewater pressures, even occurring preceding liquefaction triggering. Dilation in the 25ABCD model reduces instability and stiffens the soil column. The stronger dilatancy in the 25ABCD sand is attributed to the denser packing of the particles, where for the  $D_r\!=\!63\%$  test density the void ratios for the 100A and 25ABCD sands are 0.69 and 0.39, respectively.

While both sands liquefied, the typical co-occurring definitions of liquefaction of  $r_u \! = \! 1.0$  and  $\gamma \! = \! 3\%$  (Idriss and Boulanger 2008) were not coincident in the 25ABCD sand. The lower magnitude of shear strains at triggering and the only minor accumulation during cyclic mobility reduced the consequences of liquefaction. This illustrates that the dynamic performance of poorly graded sands is different from well graded sands and assuming identical responses may result in overly conservative seismic designs of embankments.

# 6 CONCLUSIONS

A centrifuge experiment to study the effects of gradation on the response of saturated sands during earthquake shaking was presented. Using inverse analysis procedures and recorded in-situ accelerations, stress-strain responses for the test sands were calculated using pseudo-elements and compared. The following are the main observations.

- Inverse analysis procedures are an effective tool for evaluating local soil dynamic behaviors in a centrifuge experiment. Calculated stress-strain behaviors better match field conditions (e.g., capturing true dynamic effects or upward seepage) and responses are not strongly inhibited by boundary effects present in laboratory testing.
- Liquefaction was triggered in both sands, but the well graded sand (25ABCD) had stronger stress-dilatancy behavior than the poorly graded sand (100A). As a result, shear strains in the well graded sand accumulated at a slower rate and the maximum strain was about 30% of the strain measured in poorly graded sand.
- An excess porewater pressure ratio of 1.0 and 3% shear strain may not occur simultaneously in liquefying well graded sands. Well graded sands require a greater number of loading cycles to reach 3% shear strains relative to poorly graded soils.
- A clean sand assumption may not be appropriate for well graded sands and may result in overly conservative embankment designs. Additional gradation properties (e.g. void ratio) should be considered during liquefaction assessment.

## **ACKNOWLEDGEMENTS**

The National Science Foundation (NSF) provided the funding for this work under grant No. CMMI-1916152 and also funded the Natural Hazards Engineering Research Infrastructure (NHERI) shared use centrifuge facility at the University of California at Davis under grant No. CMMI-1520581. Any opinions, findings and conclusions or recommendations expressed in this material are those of the author(s) and do not necessarily reflect those of the NSF. The authors would also like to thank Dan Wilson, Alejandro Martinez, Rachel Reardon, Francisco Humire, Mandeep Singh Basson, and Sheikh Sharif Ahmed, for their insights and recommendations. The successful centrifuge experiment was made possible by the UC Davis Center for Geotechnical Modeling (CGM) staff.

### **REFERENCES**

Andrus, R.D. and Youd, T.L. 1987. Subsurface Investigation of a Liquefaction-Induced Lateral Spread, Thousand Springs Valley, Idaho. Report to U. S. Army Corps of Engineers, miscellaneous paper GL-87-8, Dept. of Civil Eng., Brigham Young Univ. Provo, UT.

Boulanger, R.W. and Idriss, I.M. 2014. CPT and SPT based liquefaction triggering procedures. Report No. UCD/CGM-14/01, Center for Geotechnical Modeling, Department of Civil and Environmental Engineering, University of California, Davis, CA, 134 pp.

Brandenberg, S.J., Wilson, D.W., and Rashid, M.M. 2010. A weighted residual numerical differentiation algorithm applied to experimental bending moment data. *Journal of Geotechnical and Geoenvironmental Engineering*, 136, 854-863

- Garnier, J., Gaudin, C., Springman, S.M., Culligan, P.J., Goodings, D., Konig, D., Kutter, B., Phillips, R., Randolph, M.F., and Thorel, L. 2007. Catalogue of scaling laws and similitude questions in geotechnical centrifuge modelling. *International Journal of Physical Modelling in Geotechnics*, 7(3), 1–23.
- Ghafghazi M. and DeJong J.T. 2016. A Review of Liquefaction Case Histories in Gravelly Soils Using SPT-Based Triggering Curves. *GeoVancouver 2016*, Canadian Geotechnical Society, Vancouver, BC, Canada
- Idriss, I.M. and Boulanger, R.W. 2008. *Soil Liquefaction During Earthquakes*, Oakland, CA, Earthquake Engineering Research Institute.
- Kamai, R. and Boulanger, R.W. 2010. Characterizing localization processes during liquefaction using inverse analyses of instrumentation arrays, Meso-scale shear physics in earthquake and landslide mechanics, 219-238.
- Kutter, B.L. and Wilson D.W. 1999. De-Liquefaction Shock Waves. 7<sup>th</sup> US-Japan Workshop on Earthquake Resistant Design of Lifeline Facilities and Countermeasures Against Soil Liquefaction. Buffalo, NY, USA.
- Sturm, A.P. 2019. On the Liquefaction Potential of Gravelly Soils: Characterization, Triggering and Performance. PhD Dissertation. University of California, Davis.
- Towhata, I., Maruyama, S., Kasuda, K. I., Koseki, J., Wakamatsu, K., Kiku, H., Kiyota, T., Yasuda, S., Taguchi, Y., Aoyama, S., and Hayashida, T. 2014. Liquefaction in the Kanto region during the 2011 off the pacific coast of Tohoku earthquake, *Soils and Foundations*, 54(4), 859–873.